

An Automatic 40-Wavelength Channelized Equalizer

C. R. Doerr, *Member, IEEE*, L. W. Stulz, R. Pafchek, L. Gomez, M. Cappuzzo, A. Paunescu, E. Laskowski, L. Buhl, H. K. Kim, and S. Chandrasekhar

Abstract—We demonstrate a wavelength equalizer in planar silica waveguides that can automatically control individual channel powers in a 40-channel 100-GHz-channel-spacing wavelength-division multiplexed system, yet gives no distortion to channels that already have the same power as their neighbors. It has <6.8 dB insertion loss over 32-nm, 9–13-dB attenuation range, and <0.18 dB polarization/time-dependent loss.

Index Terms—Couplers, equalizers, gain control, glass materials/devices, gratings, wavelength division multiplexing.

I. INTRODUCTION

IN LARGE channel-count wavelength-division multiplexed (WDM) networks, it is important to insure that none of the channels becomes significantly weaker than the others, otherwise its reduced optical signal-to-noise ratio could result in transmission penalties. Recently, several dynamic filters have been demonstrated that can equalize the gain of optical amplifiers but cannot control individual channel powers [1]–[6]. There have been some demonstrations of dynamic channelized filters [7]–[10], but these impose filtering on channels that do not need adjustment relative to their neighbors, limiting the allowable number of equalizers in the transmission line. Here, we present a dynamic filter that can adjust the transmissivity for each channel independently as well as provide distortion-free transmission when desired.

II. DESIGN

The equalizer is made in silica waveguides on a silicon substrate. The waveguide core index is $\sim 0.65\%$ higher than the cladding. The design (see Fig. 1) is a Mach–Zehnder interferometer with a grating–lens–grating cascade in one arm [5]. We will call this arm the filtered arm, and the other, the nonfiltered arm. The interferometer employs $\sim 50/50$ evanescent couplers and is in the cross-state (one fiber is glued to an upper input and the other to a lower) to reduce the wavelength dependence and fabrication uncertainty of the couplers. The gratings have 60 waveguides each, and there are 61 lens inlets per grating free-spectral range, the central 44 of which on each side are connected to each other by equal-length waveguides. Thus the optical spectrum is slightly oversampled, allowing the device to perfectly reconstruct the input spectrum over the band of interest, if so desired [5]. Each lens waveguide, as well as the nonfiltered arm, contains a thermo-optic phase shifter, consisting of a chrome heater ($3.8 \text{ mm} \times 38 \text{ }\mu\text{m}$) over the waveguide. The phase shifters are spaced by $100 \text{ }\mu\text{m}$.

Manuscript received March 29, 2000; revised May 3, 2000.

The authors are with Bell Laboratories, Lucent Technologies, Holmdel, NJ 07733 USA (e-mail: crdoerr@lucent.com).

Publisher Item Identifier S 1041-1135(00)07456-5.

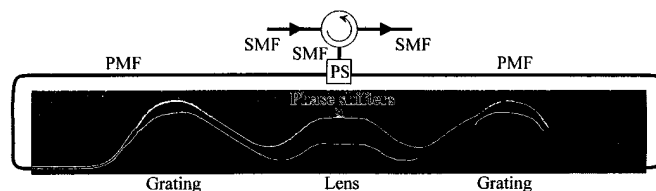


Fig. 1. Channelized equalizer. PMF = polarization maintaining fiber, SMF = single-mode fiber, and PS = polarization splitter.

Wafer real estate is precious for this long 44-channel device. A significant fraction of the physical size is the star couplers. The radiating waveguides from the star couplers must reach a certain spacing before they can bend in the gratings and lens. As explained in [11], the smaller the inlet center-to-center spacing at the star coupler edges, $10 \text{ }\mu\text{m}$ in the case here, the smaller the star coupler. A small spacing results in significant mutual coupling among the inlets. The mutual coupling results in a mainly periodic phase distortion in the star coupler, for which we compensate by appropriately lengthening the grating and lens outer arms. Fig. 2(a) shows the path-length correction, and Fig. 2(b) shows the calculated transmissivity from the input of one of the waveguide gratings to one of the central lens arms for with (solid line) and without (dashed line) the path-length correction. As one can see, the path-length correction keeps the passband narrow, despite the mutual coupling among the lens inlets, maximizing the optical isolation between the equalizer controls.

The circuit has high polarization-dependent loss (PDL). This is because of difference in strain and shape birefringence between the filtered and nonfiltered arms and also strain birefringence in the gratings. This PDL can be reduced through various known techniques, but it is difficult to reach the $\sim 0.1\text{-dB}$ PDL specification required for many long-haul systems. However, by using a circulator, a polarization splitter, and polarization-maintaining fiber between the device and the splitter oriented such that only one polarization exists on the chip, one has extremely low PDL without having to do anything to the circuit (see Fig. 1). For the device described here, all the light on the chip is transverse-magnetic polarized. Another advantage to this scheme is that it also eliminates the polarization-mode dispersion (PMD) of the chip. A silica chip typically has a strain-induced birefringence of $\sim 2 \times 10^{-4}$. Thus a 15-cm-path-length chip that does not use the above scheme would have $\sim 0.15 \text{ ps}$ of PMD. Note that this method of PDL elimination is advantageous over the method of using a circulator on one side and a Faraday mirror on the other. This is because in this latter method, PDL in the chip will increase the insertion loss and/or reduce the dynamic range, any fiber-coupling losses are paid for twice, and for a given dynamic range, a single-pass version of the single-filtered-arm interferometer can have lower loss than a double-pass

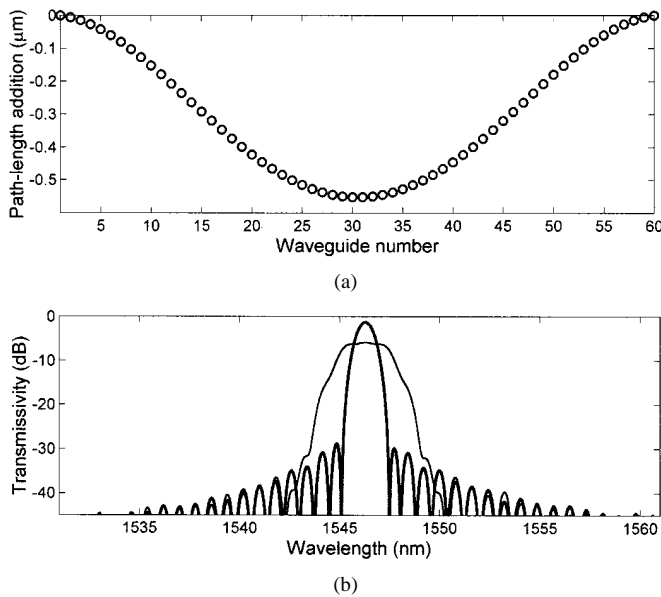


Fig. 2. (a) Path-length correction in the gratings and lens for mutual coupling in the star-coupler inlets. (b) Calculated transmissivity from the input of the grating to a central lens arm for with (solid) and without (dashed) the path-length correction.

version (via adjustment of the coupler ratios). One can verify this last point by considering the case of infinite dynamic range: in such a case the design will be the same whether it is single-pass or double-pass, yet the single-pass version will have lower loss.

III. RESULTS

The chip is $1.4 \text{ cm} \times 11 \text{ cm}$. Its center is soldered to a copper block, and each grating has its own resistive heater and temperature sensor and is not in contact with anything but air. This is because the gratings shift by $0.01 \text{ nm}/^\circ\text{C}$. Via a 50-pin SCSI connector, the device is connected to 45 12-bit computer-controlled voltage drivers. It takes $\sim 425 \text{ mW}$ to shift a phase shifter by π . The two gratings are wavelength-aligned when at the same temperature.

The coupling ratios of the two evanescent couplers turned out to be $\sim 60/40$. However, because the interferometer is in the cross state, the net effect is 50/50 couplers, with 0.2-dB excess device loss. The insertion loss and attenuation range of the equalizer are shown in Fig. 3. The top and bottom smooth traces were obtained by adjusting all of the phase shifters for maximum and minimum transmissivity, respectively. One can see that the insertion loss is $< 6.8 \text{ dB}$ over 32 nm; $\sim 2.8 \text{ dB}$ of this is from the circulator and polarization splitter. The upper and lower curves with the dip and peak were obtained by adjusting control no. 23 by π and not adjusting any other phase shifter. As one can see, the thermal crosstalk between controls is small, although nonzero. One can also see that the optical crosstalk between controls is small, as explained in Section II. Also, the available attenuation range is less ($\sim 9 \text{ dB}$) when a solitary control is changed compared to when its neighbors follow it ($\sim 13 \text{ dB}$). This is due to the spectral overlap of the control points. The polarization/time-dependent loss is $< 0.18 \text{ dB}$,

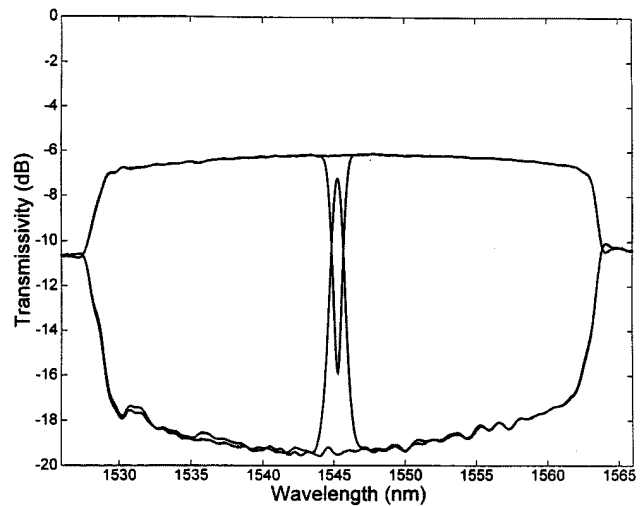


Fig. 3. Measured transmissivity through the equalizer (including the circulator and polarization splitter) for various conditions of the phase shifters.

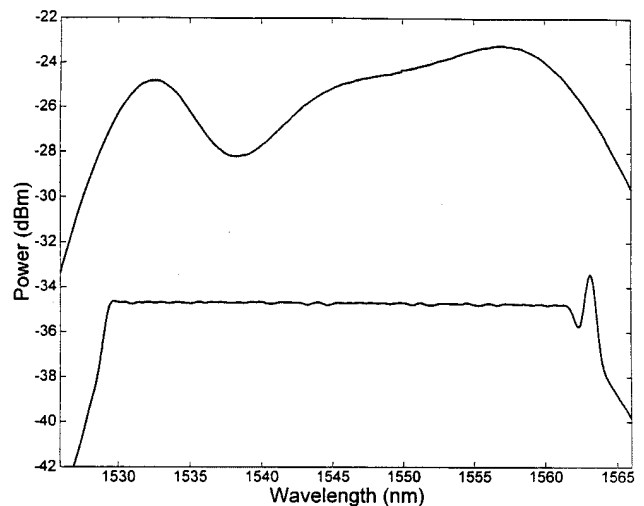


Fig. 4. Measured result of automatic flattening of an amplified spontaneous emission spectrum. The upper is the spectrum before the equalizer, and the lower is after the equalizer.

this particular chip, but was measured for other chips of the same general design and was found to be below $\pm 0.6 \text{ ps/nm}$. It is so small because all of the path-lengths for all of the wavelengths are the same to within a wavelength. The response time of each control is $\sim 2 \text{ ms}$, although if there is a sudden large change in total electrical driving power, there is a small settling on the order of a minute.

Because we used the equal-straight-bend design for the lens waveguides [12], the lens-arm phases are well-aligned in the zero-power condition. Thus the power consumption is $\sim 5 \text{ W}$ for relatively smooth desired filter shapes. The power consumption increases as the channel disorder increases. The highest power consumption condition is equalizing the case of 20 channels 9–13 dB lower than the other 20. Ideally, the total power consumption for this would be $\sim 8.5 \text{ W}$. In reality, we have seen cases up to $\sim 12 \text{ W}$.

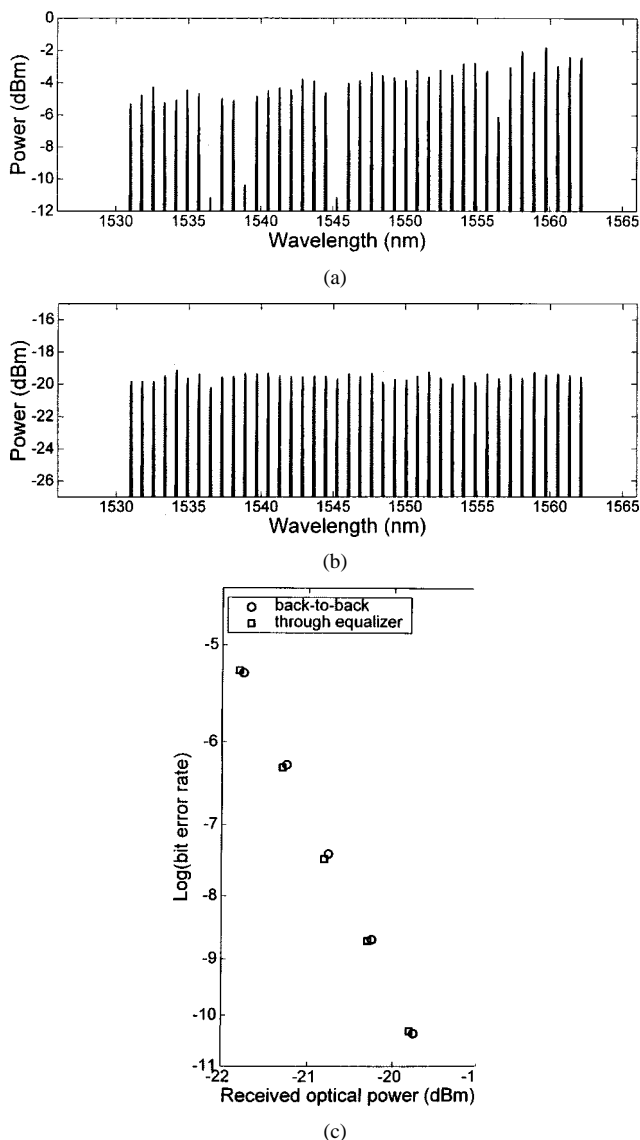


Fig. 5. Measured result of automatic equalization of 40 laser channels with unequal channel powers. (a) Before the equalizer. (b) After the equalizer. (c) Bit-error rate curve of an OC-192 signal, pattern length $2^{31} - 1$, before and after the equalizer.

works as follows: after the device is packaged, it must be calibrated. Using an optical noise source and an OSA, the maximum transmissivity condition for all controls simultaneously is found. Then the program finds the differences between the control and nonfiltered electrical powers to obtain a maximum and minimum for each control point and its wavelength center, and stores these values in a file. Then when used as an equalizer, it takes a scan from the OSA, looks in a wavelength band centered

around each control point, and adjusts the voltage for that control up or down appropriately, insuring that the electrical power difference between the control and the nonfiltered stays within the limits found in the calibration. Using this feedback system, we automatically equalized an amplified spontaneous emission spectrum (Fig. 4) and 40 laser peaks, with an initial deviation of up to 9 dB (Fig. 5) (only the central 42 controls were used). To verify that the filter has no transmission impairments, we modulated one of the laser peaks at 10 Gb/s, and we observed no penalty, as shown in Fig. 5(c).

ACKNOWLEDGMENT

The authors thank M. Zirngibl, A. E. White, G. Bogert, W. Minford, P. Bernasconi, J. Fernandes, W. Shieh, and S. Patel.

REFERENCES

- [1] K. Inoue, T. Kominato, and H. Toba, "Tunable gain equalization using a Mach-Zehnder optical filter in multistage fiber amplifiers," *IEEE Photon. Technol. Lett.*, vol. 3, pp. 718–720, 1991.
- [2] S. H. Huang, X. Y. Zou, S.-M. Hwang, A. E. Willner, Z. Bao, and D. A. Smith, "Experimental demonstration of dynamic network equalization of three 2.5 Gb/s WDM channels over 1000 km using acoustooptic tunable filters," *IEEE Photon. Technol. Lett.*, vol. 8, pp. 1243–1245, 1996.
- [3] H. S. Kim, S. H. Yun, H. K. Kim, N. Park, and B. Y. Kim, "Actively gain-flattened erbium-doped fiber amplifier over 35 nm by using all-fiber acousto-optic tunable filters," *IEEE Photon. Technol. Lett.*, vol. 10, pp. 790–792, 1998.
- [4] J. E. Ford and J. A. Walker, "Dynamic spectral power equalization using micro-optomechanics," *IEEE Photon. Technol. Lett.*, vol. 10, pp. 1440–1442, 1998.
- [5] C. R. Doerr, M. Cappuzzo, E. Laskowski, A. Paunescu, L. Gomez, L. W. Stulz, and J. Gates, "Dynamic wavelength equalizer in silica using the single-filtered-arm interferometer," *IEEE Photon. Technol. Lett.*, vol. 11, pp. 581–583, 1999.
- [6] B. J. Offrein, G. L. Bona, R. Germann, F. Horst, and H. W. M. Salemink, "Dynamic gain equalizer in high-index-contrast SiON technology," in *ECOC (Post Deadline Paper)*, 1999, pp. 6–7.
- [7] M. Zirngibl, C. H. Joyner, and B. Glance, "Digitally tunable channel dropping filter/equalizer based on waveguide grating router and optical amplifier integration," *IEEE Photon. Technol. Lett.*, vol. 6, pp. 513–515, 1994.
- [8] M. C. Parker, A. D. Cohen, and R. J. Mears, "Dynamic holographic spectral equalization for WDM," *IEEE Photon. Technol. Lett.*, vol. 9, pp. 529–530, 1997.
- [9] J.-X. Cai, K.-M. Feng, X. Chen, A. E. Willner, D. A. Smith, C.-H. Lee, and Y.-J. Chen, "Experimental demonstration of dynamic high-speed equalization of three WDM channels using acousto-optic modulators and a wavelength demultiplexer," *IEEE Photon. Technol. Lett.*, vol. 9, pp. 678–680, 1997.
- [10] R. Giles, D. Bishop, V. Aksyuk, A. Dentai, R. Ruel, and E. Burrows, "Low-loss channelized WDM spectral equalizer using lightwave micro-machines and autonomous power regulation," presented at the Optical Fiber Communication Conf., PD31, 1999.
- [11] C. R. Doerr, "Cascaded planar waveguide arrays," *Trends in Optics and Photonics*, vol. 29, 1999.
- [12] C. R. Doerr and C. Dragone, "Proposed optical cross-connect using a planar arrangement of beam steerers," *IEEE Photon. Technol. Lett.*, vol. 11, pp. 197–199, 1999.